

8-21-2013

A Supramolecular Strategy to Assemble Multifunctional Viral Nanoparticles

Limin Chen
Chinese Academy of Sciences


Xia Zhao
Chinese Academy of Sciences

Yuan Lin
Chinese Academy of Sciences, linyuan@ciac.jl.cn

Yubin Huang
Chinese Academy of Sciences

Qian Wang
University of South Carolina - Columbia, wang@mail.chem.sc.edu

Follow this and additional works at: https://scholarcommons.sc.edu/chem_facpub

 Part of the [Biochemistry Commons](#), [Immunology of Infectious Disease Commons](#), [Medicinal-Pharmaceutical Chemistry Commons](#), [Organic Chemistry Commons](#), [Virology Commons](#), and the [Virus Diseases Commons](#)

Publication Info

Published in *Chemical Communications*, Volume 49, Issue 83, 2013, pages 9678-9680.
© [Chemical Communications](#) 2013, Royal Society of Chemistry.

This Article is brought to you by the Chemistry and Biochemistry, Department of at Scholar Commons. It has been accepted for inclusion in Faculty Publications by an authorized administrator of Scholar Commons. For more information, please contact dillarda@mailbox.sc.edu.

A supramolecular strategy to assemble multifunctional viral nanoparticles†

Limin Chen,^a Xia Zhao,^a Yuan Lin,^{*a} Yubin Huang^a and Qian Wang^{*ab}

Cite this: *Chem. Commun.*, 2013, **49**, 9678

Received 22nd July 2013,
Accepted 21st August 2013

DOI: 10.1039/c3cc45559a

www.rsc.org/chemcomm

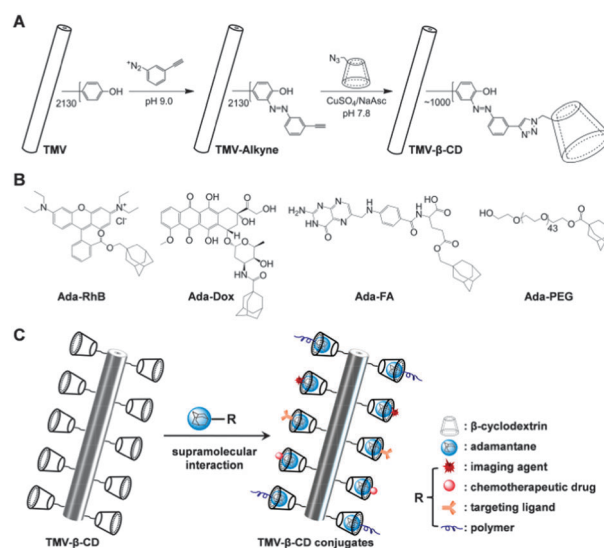
Using a one-pot approach driven by the supramolecular interaction between β -cyclodextrin and adamantyl moieties, multifunctional viral nanoparticles can be facily formulated for biomedical applications.

The development of multifunctional nanoparticles for biomedical applications is of great importance.^{1,2} For example, the development of theranostic nanoparticles loaded with therapeutic drugs and imaging probes for the combined therapy and diagnosis has been gaining wide interest.^{3,4} Recently, inspired by the hierarchical structures of biogenic viral particles, multifunctional virus-like nanostructures have been constructed from synthetic polymers.^{5,6} In the meantime, the application of viral nanoparticles (VNPs) derived from plants and bacteria in biomedical fields has also attracted great attention, primarily due to their well-defined, programmable, multivalent and monodispersed structural features^{7–19} as well as their good biocompatibility.^{20,21} To make the best use of the inherent compositions and structures of VNPs, many multifunctional VNPs have been constructed by the combination of mutagenesis and bioconjugation approaches, by which a variety of targeting ligands, catalytic units, diagnostic probes and therapeutic cargos have been anchored on the surface or inside of the internal cavity of VNPs.^{12,22–29}

On the other hand, supramolecular interactions have been extensively applied to constructing drug and gene delivery systems, as well as smart materials due to their modularity, reversibility and stimuli-responsiveness.^{30–36} For example, β -cyclodextrin (β -CD), a natural toroid-shaped cyclic oligosaccharide, is one of the most widely used host-systems in supramolecular chemistry thanks to its low cost, good water solubility and biocompatible properties.³⁷ β -CD has a hydrophilic exterior surface and a hydrophobic interior cavity that can accommodate a broad range of guest molecules (e.g., adamantane, azobenzene, and ferrocene).^{38,39}

In this work, the supramolecular interaction between β -CD and adamantyl (Ada) moieties was exploited to assemble multifunctional VNPs. Tobacco mosaic virus (TMV) was employed as a model VNP, which is a classic example of rod-shaped plant virus, 300 nm long and 18 nm in diameter, consisting of 2130 identical subunit proteins arranged helically around genomic single RNA strand. β -CD units could be grafted onto the exterior surface of TMV using efficient bioconjugation reactions; and folic acid (FA), rhodamine B (RhB), doxorubicin (Dox), and polyethylene glycol (PEG) (M_w 2000 Da) were selected to functionalize TMV particles upon derivatization with Ada moieties and sequential supramolecular assembly (Scheme 1).

As shown in Scheme 1A, β -CD was attached to the exterior surface of TMV by sequential diazonium-coupling and Cu^I-catalyzed azide-alkyne cycloaddition (CuAAC) reactions.^{40,41} β -CD-azide was synthesized using a reported protocol,⁴² and the CuAAC reaction was catalyzed with CuSO₄ and sodium ascorbate (NaAsc).⁴³



Scheme 1 (A) Synthesis of TMV- β -CD by diazonium-coupling and CuAAC reactions. (B) The structures of Ada derivatives. (C) Schematic demonstration of the formation of multifunctional TMV via the supramolecular interaction between β -CD and Ada moieties.

^a State Key Laboratory of Polymer Physics and Chemistry, Changchun Institute of Applied Chemistry, Chinese Academy of Sciences, Changchun, 130022, P. R. China. E-mail: linyuan@ciac.jl.cn, wang263@mailbox.sc.edu

^b Department of Chemistry and Biochemistry, University of South Carolina, Columbia, South Carolina 29208, USA

† Electronic supplementary information (ESI) available: Preparation of β -CD-azide, Ada derivatives and TMV- β -CD conjugates and experimental details of cellular uptake and cytotoxicity. See DOI: 10.1039/c3cc45559a

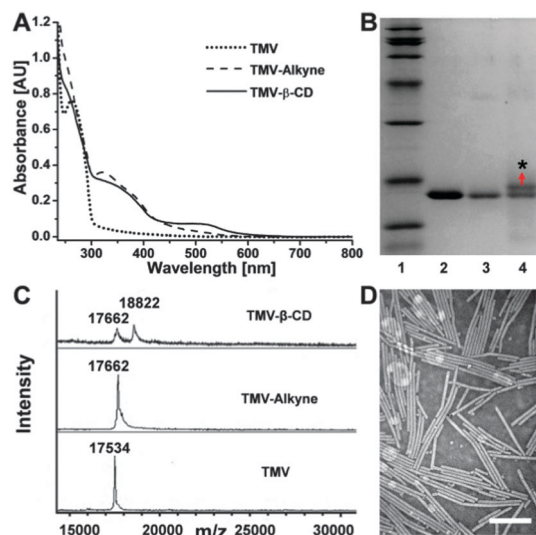


Fig. 1 Characterization of **TMV-β-CD**. (A) UV-Vis spectra of **TMV**, **TMV-Alkyne** and **TMV-β-CD**. (B) SDS-PAGE: lane 1, protein markers; lane 2, **TMV**; lane 3, **TMV-Alkyne**; lane 4, **TMV-β-CD** (* indicates the **TMV-β-CD** capsid monomer). (C) MALDI-TOF MS of the subunit proteins of **TMV** (m/z 17 534), **TMV-Alkyne** (m/z 17 662) and **TMV-β-CD** (m/z 18 822, the 1160 m/z difference between **TMV-β-CD** and **TMV-Alkyne** is consistent with the theoretical molar mass of newly added β-CD-azide). (D) TEM image of uranyl acetate-stained **TMV-β-CD**. The scale bar is 200 nm.

The formation of **TMV-Alkyne** was confirmed by UV-Vis spectroscopy (Fig. 1A) and MALDI-TOF MS (Fig. 1C). The UV-Vis spectrum of **TMV-β-CD** shows a new absorption peak at 510 nm in company with a significant decrease in absorbance at 330 nm compared to the spectrum of **TMV-Alkyne**, which can be attributed to the conjugative effect between the azobenzenyl and 1,2,3-triazol moieties, implying a successful attachment of β-CD moieties by the CuAAC reaction. This can also be verified by the SDS-PAGE analysis (Fig. 1B). The grafting efficiency was roughly estimated to be about 50% based on band density analysis of **TMV-β-CD** subunit proteins *versus* **TMV-Alkyne** subunit proteins, indicating that every **TMV** particle has about 1000 β-CD units, which is consistent with the MALDI-TOF MS result (Fig. 1C). Increasing the concentration of β-CD-azide did not improve the grafting density, which saturated at ~50% (Fig. S1, ESI†). We hypothesize that the incomplete conjugation is due to the steric hindrance of the β-CD moieties. Finally, the integrity of the **TMV** particles upon conjugation was confirmed using transmission electron microscopy (TEM, Fig. 1D).

To test the supramolecular interaction between β-CD and Ada moieties, a series of Ada derivatives were synthesized by either esterification or amidation reactions following literature protocols (see ESI† for experimental details). As a typical protocol, **TMV-β-CD** was incubated with a 10-fold molar excess of **Ada-RhB** relative to the subunit proteins for 30 min at 4 °C, followed by dialysis and ultracentrifugation affording **TMV-β-CD/Ada-RhB**, which was confirmed by size-exclusion chromatography (SEC) analysis (Fig. 2A). The SEC diagram shows that the retention volume of **TMV-β-CD/Ada-RhB** is identical to that of **TMV-β-CD**; however, a significantly enhanced absorbance at 568 nm is observed due to the encapsulation with **Ada-RhB**. In comparison, the control experiment following the identical protocol but using unmodified **TMV** did not show any non-specific interactions

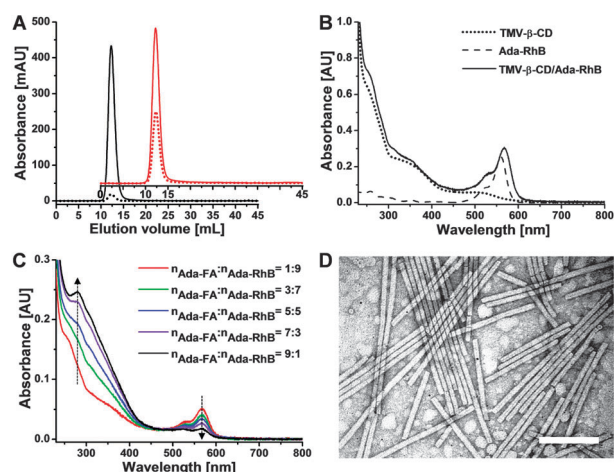


Fig. 2 (A) SEC diagram of **TMV-β-CD/Ada-RhB** (red) and **TMV-β-CD** (black) monitored at 260 nm (solid) and 568 nm (dot). (B) UV-Vis spectra of **TMV-β-CD**, **Ada-RhB** and **TMV-β-CD/Ada-RhB**. (C) UV-Vis spectra of **TMV-β-CD/Ada-FA/Ada-RhB** with varying molar ratios of **Ada-FA** and **Ada-RhB** ($n_{\text{Ada-FA}}:n_{\text{Ada-RhB}}$) used. (D) TEM image of uranyl acetate-stained **TMV-β-CD/Ada-FA/Ada-RhB** ($n_{\text{Ada-FA}}:n_{\text{Ada-RhB}} = 1:9$). The scale bar is 200 nm.

with **Ada-RhB** as confirmed by SEC analysis (Fig. S2A, ESI†). The results validated that **TMV-β-CD** can assemble with **Ada-RhB** *via* the interaction between β-CD and Ada groups.

The eluted **TMV-β-CD/Ada-RhB** fraction was subjected to UV-Vis spectroscopy assay (Fig. 2B), and the labeling efficiency was calculated based on typical absorbance of **TMV-β-CD** and **Ada-RhB**. The yield was ~100%, indicating that all β-CD units were quantitatively filled with Ada moieties, *i.e.* each **TMV-β-CD** particle was complexed with ~1000 **Ada-RhB** molecules (see ESI† for details). Furthermore, the integrity of **TMV-β-CD/Ada-RhB** was confirmed using TEM (Fig. S2B, ESI†). It is noteworthy that the positively charged **Ada-RhB** did not induce the aggregation and precipitation of **TMV-β-CD** particles. Following the identical procedure, **TMV-β-CD/Ada-Dox** (or **Ada-FA**, **Ada-PEG-RhB**) can be readily achieved (Fig. S3–S5, ESI†). Each **TMV-β-CD** particle can accommodate ~1000 **Ada-Dox** and **Ada-FA** molecules but only ~700 **Ada-PEG-RhB** molecules due to the steric hindrance.

To test the one-pot co-assembly behavior between **TMV-β-CD** and different Ada derivatives, **TMV-β-CD/Ada-FA/Ada-RhB** was prepared following the typical protocol. The UV-Vis spectra show that the absorbance of **Ada-FA** ($\lambda_{280\text{nm}}$) gradually increases in company with the decrease in the absorbance of **Ada-RhB** ($\lambda_{568\text{nm}}$) as various molar ratios of **Ada-FA** and **Ada-RhB** from 1:9 to 9:1 were used (Fig. 2C). Based on the UV-Vis spectrum, the average number of **Ada-FA** and **Ada-RhB** moieties per **TMV-β-CD** particle can be determined accordingly (see ESI†), and the results are given in Fig. S6C, ESI†. According to the TEM results (Fig. 1D and 2D), there were no significant changes in length and diameter of **TMV** particles after being grafted with β-CD and sequential assembly. **TMV-β-CD/Ada-FA/Ada-Dox** can also be prepared following the same protocol (Fig. S6, ESI†).

In vitro drug release kinetics showed that **Ada-Dox** released in a sustained manner due to the dissociation of the β-CD/Ada supramolecular structure (Fig. S7, ESI†), similar to the literature reports.^{31,32,36} To investigate the selective targeting ability of Dox-loaded **TMV**, HepG2 tumor cells (folate receptor positive) and NIH-3T3 fibroblast

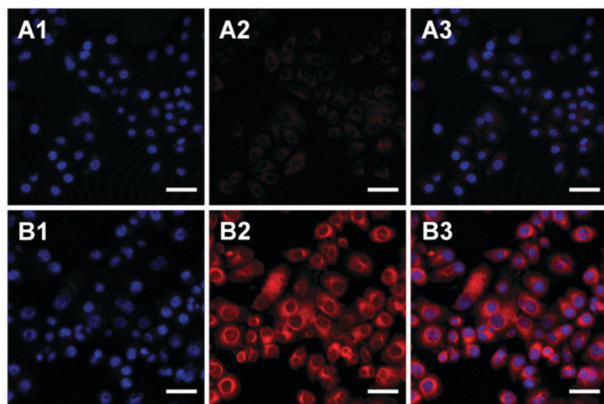


Fig. 3 Fluorescent microscopy images of HepG2 cells. (A and B) HepG2 cells incubated with **TMV-β-CD/Ada-Dox** and **TMV-β-CD/Ada-FA/Ada-Dox** for 24 h, respectively. 1, 2 and 3 indicate the DAPI, **Ada-Dox** and merged channels, respectively. The scale bars represent 50 μm.

cells (folate receptor negative) were treated with **TMV-β-CD/Ada-Dox**, **TMV-β-CD/Ada-FA/Ada-Dox** and free Dox. Cellular uptake and cell proliferation were evaluated by confocal laser scanning microscopy and cell viability assay, respectively. As shown in Fig. 3 and Fig. S8 (ESI[†]), the two types of Dox-loaded TMV showed low red fluorescence in NIH-3T3 cells, while **TMV-β-CD/Ada-FA/Ada-Dox** showed much stronger red fluorescence in HepG2 cells compared to **TMV-β-CD/Ada-Dox**. It indicated that the folate receptor-mediated endocytosis enhanced the intracellular drug delivery. As shown in Fig. S9 (ESI[†]), the two types of Dox-loaded TMV significantly decreased the cytotoxicity of Dox against NIH-3T3 cells, while **TMV-β-CD/Ada-FA/Ada-Dox** showed much higher cytotoxicity against HepG2 cells than **TMV-β-CD/Ada-Dox**, which was comparable to that of free Dox. It demonstrated that Dox-loaded TMV with the aid of FA moieties showed noticeable antitumor selectivity compared to free Dox. The **TMV-β-CD/Ada-FA/Ada-Dox** particles afforded comparable therapy efficiency of free Dox towards HepG2 cells, confirming the potential for sustained release of Dox due to the dissociation of the β-CD/Ada supramolecular structure.^{31,32}

In summary, we have demonstrated here a supramolecular strategy based on the interaction between β-CD and Ada moieties. Using this method, multifunctional TMV particles have been constructed in a facile manner to load with imaging agents, targeting ligands, and chemotherapeutic drugs, which could potentially be used in therapeutic and diagnostic applications. More importantly, based on this work, we expect that a broad range of stimuli-responsive supramolecular interactions can be combined with VNPs for versatile applications.

This work was supported by the National Natural Science Foundation of China (21128002 and 21104080).

Notes and references

- 1 J. Nicolas, S. Mura, D. Brambilla, N. Mackiewicz and P. Couvreur, *Chem. Soc. Rev.*, 2013, **42**, 1147–1235.
- 2 M. Elsabahy and K. L. Wooley, *Chem. Soc. Rev.*, 2012, **41**, 2545–2561.
- 3 A. M. Nystrom and K. L. Wooley, *Acc. Chem. Res.*, 2011, **44**, 969–978.
- 4 J. Zhuang, M. R. Gordon, J. Ventura, L. Li and S. Thayumanavan, *Chem. Soc. Rev.*, 2013, **42**, 7421–7435.
- 5 M. Elsabahy, R. Shrestha, C. Clark, S. Taylor, J. Leonard and K. L. Wooley, *Nano Lett.*, 2013, **13**, 2172–2181.
- 6 R. Shrestha, M. Elsabahy, H. Luehmann, S. Samarajeewa, S. Florez-Malaver, N. S. Lee, M. J. Welch, Y. Liu and K. L. Wooley, *J. Am. Chem. Soc.*, 2012, **134**, 17362–17365.
- 7 Y. Ma, R. J. M. Nolte and J. J. L. M. Cornelissen, *Adv. Drug Delivery Rev.*, 2012, **64**, 811–825.
- 8 H. N. Barnhill, S. Claudel-Gillet, R. Ziesel, L. J. Charbonniere and Q. Wang, *J. Am. Chem. Soc.*, 2007, **129**, 7799–7806.
- 9 A. A. Aljabali, S. Shukla, G. P. Lomonossoff, N. F. Steinmetz and D. J. Evans, *Mol. Pharmaceutics*, 2013, **10**, 3–10.
- 10 Z. Yin, H. G. Nguyen, S. Chowdhury, P. Bentley, M. A. Bruckman, A. Miermont, J. C. Gildersleeve, Q. Wang and X. Huang, *Bioconjugate Chem.*, 2012, **23**, 1694–1703.
- 11 N. F. Steinmetz, A. L. Ablack, J. L. Hickey, J. Ablack, B. Manocha, J. S. Mymryk, L. G. Luyt and J. D. Lewis, *Small*, 2011, **7**, 1664–1672.
- 12 Z. Niu, M. A. Bruckman, V. S. Kotakadi, J. He, T. Emrick, T. P. Russell, L. Yang and Q. Wang, *Chem. Commun.*, 2006, 3019–3021.
- 13 J. K. Pokorski, K. Breitenkamp, L. O. Liepold, S. Qazi and M. G. Finn, *J. Am. Chem. Soc.*, 2011, **133**, 9242–9245.
- 14 Q. Zeng, T. Li, B. Cash, S. Li, F. Xie and Q. Wang, *Chem. Commun.*, 2007, 1453–1455.
- 15 K. Li, Y. Chen, S. Li, H. G. Nguyen, Z. Niu, S. You, C. M. Mello, X. Lu and Q. Wang, *Bioconjugate Chem.*, 2010, **21**, 1369–1377.
- 16 H. S. Leong, N. F. Steinmetz, A. Ablack, G. Destito, A. Zijlstra, H. Stuhlmann, M. Manchester and J. D. Lewis, *Nat. Protocols*, 2010, **5**, 1406–1417.
- 17 F. M. Brunel, J. D. Lewis, G. Destito, N. F. Steinmetz, M. Manchester, H. Stuhlmann and P. E. Dawson, *Nano Lett.*, 2010, **10**, 1093–1097.
- 18 G. Destito, R. Yeh, C. S. Rae, M. G. Finn and M. Manchester, *Chem. Biol.*, 2007, **14**, 1152–1162.
- 19 K. Zhou, F. Li, G. Dai, C. Meng and Q. Wang, *Biomacromolecules*, 2013, **14**, 2593–2600.
- 20 P. Singh, D. Prasuhn, R. M. Yeh, G. Destito, C. S. Rae, K. Osborn, M. G. Finn and M. Manchester, *J. Controlled Release*, 2007, **120**, 41–50.
- 21 G. Kaur, M. T. Valarmathi, J. D. Potts, E. Jabbari, T. Sabo-Attwood and Q. Wang, *Biomaterials*, 2010, **31**, 1732–1741.
- 22 K. Li, H. G. Nguyen, X. Lu and Q. Wang, *Analyst*, 2010, **135**, 21–27.
- 23 I. Yildiz, S. Shukla and N. F. Steinmetz, *Curr. Opin. Biotechnol.*, 2011, **22**, 901–908.
- 24 Z. Su and Q. Wang, *Angew. Chem., Int. Ed.*, 2010, **49**, 10048–10050.
- 25 L. A. Lee, H. G. Nguyen and Q. Wang, *Org. Bioorg. Chem.*, 2011, **9**, 6189–6195.
- 26 Q. Wang, T. Lin, L. Tang, J. E. Johnson and M. G. Finn, *Angew. Chem., Int. Ed.*, 2002, **41**, 459–462.
- 27 P. Singh, M. J. Gonzalez and M. Manchester, *Drug Dev. Res.*, 2006, **67**, 23–41.
- 28 T. Douglas and M. Young, *Science*, 2006, **312**, 873–875.
- 29 J. D. Fiedler, S. D. Brown, J. L. Lau and M. G. Finn, *Angew. Chem., Int. Ed.*, 2010, **49**, 9648–9651.
- 30 T. Kakuta, Y. Takashima, M. Nakahata, M. Otsubo, H. Yamaguchi and A. Harada, *Adv. Mater.*, 2013, **25**, 2849–2853.
- 31 Q. Hu, W. Li, X. Hu, Q. Hu, J. Shen, X. Jin, J. Zhou, G. Tang and P. K. Chu, *Biomaterials*, 2012, **33**, 6580–6591.
- 32 H. Fan, Q. Hu, F. Xu, W. Liang, G. Tang and W. Yang, *Biomaterials*, 2012, **33**, 1428–1436.
- 33 Y. Chen, Y. Zhang and Y. Liu, *Chem. Commun.*, 2010, **46**, 5622–5633.
- 34 S. K. M. Nalluri, J. Voskuhl, J. B. Bultema, E. J. Boekema and B. J. Ravoo, *Angew. Chem., Int. Ed.*, 2011, **50**, 9747–9751.
- 35 M. Nakahata, Y. Takashima, H. Yamaguchi and A. Harada, *Nat. Commun.*, 2011, **2**, 1–6.
- 36 Q. Hu, H. Fan, Y. Ping, W. Liang, G. Tang and J. Li, *Chem. Commun.*, 2011, **47**, 5572–5574.
- 37 J. Szejtli, *Chem. Rev.*, 1998, **98**, 1743–1753.
- 38 Y. Chen and Y. Liu, *Chem. Soc. Rev.*, 2010, **39**, 495–505.
- 39 G. Chen and M. Jiang, *Chem. Soc. Rev.*, 2011, **40**, 2254–2266.
- 40 M. A. Bruckman, G. Kaur, L. A. Lee, F. Xie, J. Sepulveda, R. Breitenkamp, X. Zhang, M. Joralemon, T. P. Russell, T. Emrick and Q. Wang, *ChemBioChem*, 2008, **9**, 519–523.
- 41 T. L. Schlick, Z. Ding, E. W. Kovacs and M. B. Francis, *J. Am. Chem. Soc.*, 2005, **127**, 3718–3723.
- 42 R. C. Petter, J. S. Salek, C. T. Sikorski, G. Kumaravel and F. T. Lin, *J. Am. Chem. Soc.*, 1990, **112**, 3860–3868.
- 43 V. V. Rostovtsev, L. G. Green, V. V. Fokin and K. B. Sharpless, *Angew. Chem., Int. Ed.*, 2002, **41**, 2596–2599.